Electron photodetachment from a Dirac bubble potential. A model for the fullerene negative ion C_{60}^-

Lawrence L. Lohr and S.M. Blinder

Department of Chemistry, University of Michigan, Ann Arbor, MI 48109-1055, USA

Received 20 February 1992; in final form 20 July 1992

A model for the fullerene anion C_{60}^- is proposed in which the outer electron moves in an attractive deltafunction potential in the shape of a spherical bubble. Exact solutions for this "Dirac bubble potential" were previously worked out. On the basis of this model, the photodetachment cross-section and its angular distribution are computed as functions of photoelectron energy, for the electron in both S-like and P-like bound states. Secondary maxima and minima in the cross section appear at higher energy values, somewhat analogous to the scattering of radiation from a conducting sphere.

1. Introduction

The current high level of interest in the nearly spherical closo-polyhedral forms of carbon such as fullerene C_{60} (symmetry I_h) has prompted us to consider an exactly soluble model for such systems. Specifically we have considered an application of the "Dirac bubble potential" model to both the bound and continuum states of an electron in the open-shell anion C_{60}^-. In this model, the potential energy is represented as a Dirac delta-function in the radial coordinate r. The potential energy is assumed to equal zero for all r except $r=r_0$, at which radius it is infinitely negative, corresponding to a very short-range attractive force. Previously one of us derived exact solutions for this quantum-mechanical problem [1]. In the present study we consider an attractive bubble potential and compute, in addition to energy eigenvalues, radiative transition moments, photodetachment cross-sections and angular distribution parameters as functions of photon energy.

There are other exactly soluble spherical models which might be considered but which lack some of the desirable features of the bubble potential. The model of a particle confined to the surface of a sphere lacks the important radial degree of freedom. The spherical square well defined by $V=-V_0$ for $b<r<a$ is more realistic; the Dirac potential is, in fact, the limiting case of this well as $a\to b$ while $V_0\to\infty$. The related three-dimensional square-well potential, with $V=-V_0$ for $0\leqslant r<a$, has been applied to bound-continuum state (photodetachment) spectra of electrons trapped in metal–ammonia solutions [2]. This model, however, permits too much electron probability near the center of the sphere ($r\approx 0$) and is thus inappropriate for the C_{60}^- system.

We should note that, in common with free-electron models for conjugated systems, we are not taking account of the planar nodes in the π orbitals which these mobile electrons occupy. Moreover, since a deltafunction model cannot adequately represent the long-range Coulomb attraction, we restrict our application to an electron, bound or detached, in the field of a neutral C_{60} molecule – thus to photodetachment from C_{60}^-.

The electron affinity (EA) of C_{60}, determined by UV photoelectron spectroscopy [3], is 2.7 ± 0.1 eV. Several

Correspondence to: L.L. Lohr, Department of Chemistry, University of Michigan, Ann Arbor, MI 48109-1055, USA.

ab initio and semi-empirical computations [#1] have agreed that the LUMO of C_{60}, corresponding to the SOMO of C_{60}^-, transforms as t_{1u} in the group I_h.

2. Dirac bubble potential

The Schrödinger equation for a particle in a spherical deltafunction well can be written:

$$\left(-\frac{\hbar^2}{2m}\nabla^2+\frac{\alpha}{4\pi r_0^2}\delta(r-r_0)\right)\psi(r)=E\psi(r)\,. \tag{1}$$

Spherical symmetry allows the factorization $\psi(r)=R_{kl}(r)Y_{lm}(\theta,\phi)$. The radial equation can be rearranged to

$$\left(k^2+\frac{1}{r^2}\frac{\partial}{\partial r}r^2\frac{\partial}{\partial r}-\frac{l(l+1)}{r^2}\right)R_{kl}(r)=(\lambda/r_0)\delta(r-r_0)R_{kl}(r_0)\,, \tag{2}$$

having defined

$$E\equiv\hbar^2k^2/2m,\qquad \lambda\equiv m\alpha/2\pi\hbar^2r_0\,.$$

For negative energies we write

$$\kappa\equiv -\mathrm{i}k,\qquad E=-\hbar^2\kappa^2/2m\,.$$

Eq. (2) has been solved exactly [1] by exploiting isomorphisms with free-particle partial-wave Green functions. For $\lambda<0$, corresponding to an attractive deltafunction potential, there exists one and only one bound state for each angular momentum l for which the condition

$$|\lambda|>2l+1 \tag{3}$$

is fulfilled. There are no bound states for l values not satisfying (3). The bound-state eigenfunctions are given by

$$R_{\kappa,l}(r)=N_l i_l(\kappa r_<)k_l(\kappa r_>)\,, \tag{4}$$

where $r_>$ and $r_<$ are, respectively, the larger and smaller of r, r_0. Modified spherical Bessel functions are defined as follows [8]:

$$i_l(z)\equiv(\pi/2z)^{1/2}I_{l+1/2}(z)=\mathrm{i}^{-l}j_l(\mathrm{i}z)\,,$$

$$k_l(z)\equiv(2/\pi z)^{1/2}K_{l+1/2}(z)=-\mathrm{i}^l h_l^{(1)}(\mathrm{i}z)\,. \tag{5}$$

Those explicitly used in this paper are

$$i_0(z)=z^{-1}\sinh(z),\quad i_1(z)=z^{-1}\cosh(z)-z^{-2}\sinh(z),$$

$$k_0(z)=z^{-1}\exp(-z),\quad k_1(z)=(z^{-1}+z^{-2})\exp(-z)$$

The normalization constants for $l=0$ and $l=1$ are, respectively,

$$N_s=\left(\frac{1-(2\kappa r_0+1)\exp(-2\kappa r_0)}{4\kappa^5 r_0^2}\right)^{-1/2} \tag{6}$$

and

[#1] For a simple Hückel computation, see ref. [4]; CNDO/S, ref. [5]; SCF-DV-LD, ref. [6] and free-electron model with icosahedral crystal field, ref. [7].

$$N_p = \{[\kappa^2 r_0^2 - 3 + (2\kappa^3 r_0^3 + 5\kappa^2 r_0^2 + 6\kappa r_0 + 3)\exp(-2\kappa r_0)]/4\kappa^7 r_0^4\}^{-1/2} . \quad (7)$$

The consistency condition on eq. (3) at $r = r_0$, viz.,

$$-\lambda \kappa r_0 i_l(\kappa r_0) k_l(\kappa r_0) = 1 \quad (8)$$

provides a transcendental equation determining the bound-state eigenvalues.

Let us identify the t_{1u} orbital of C_{60}^- with a p($l=1$) bound state of our model. $E_p = -2.7$ eV corresponds to $\kappa_p = 0.4455$ bohr^{-1}. We take the mean radius of C_{60} as 3.55 Å [#2], or $r_0 = 6.709$ bohr. With these values in eq. (8), we identify $\lambda = -6.696$ in the bubble potential. This value of λ also implies the existence of a lower S bound state with $\kappa_s = 0.4985$ or $E_s = -3.38$ eV. The condition (3) admits just one other bound state, with $l=2$, $\kappa_d = 0.3256$, $E_d = -1.44$ eV.

The continuum eigenfunctions can be represented as follows:

$$R_{k,l}(r) = (2k/\pi)^{1/2}[j_l(kr_>)\cos\delta_l - y_l(kr_>)\sin\delta_l] j_l(kr_<)/j_l(kr_0) , \quad (9)$$

where j_l and y_l are spherical Bessel functions. The phase shifts δ_l are determined by

$$\cot\delta_l = \frac{y_l(kr_0)}{j_l(kr_0)} - \frac{1}{\lambda kr_0 [j_l(kr_0)]^2} . \quad (10)$$

These functions are deltafunction-normalized on the energy scale according to

$$\int_0^\infty R_{k,l}(r) R_{k',l}(r) r^2 \, dr = \delta(E - E') . \quad (11)$$

Figs. 1 and 2 show bound and continuum eigenfunctions for $l=0$ and 1. Note that these functions all have a

[#2] The authors of ref. [9] determined a mean radius of 3.532(2) Å by X-ray diffraction at 110 K; those of ref. [10] report a mean radius of 3.556(5) Å by gas-phase electron diffraction.

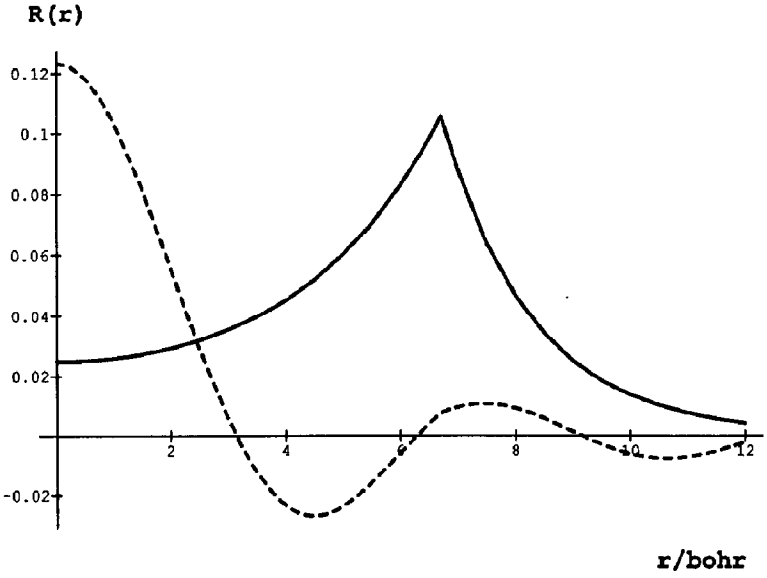

Fig. 1. Radial functions $R(r)$ for bound S state (solid curve) and continuum s state (dashed curve, 1/10 scale) with $k=1$ ($E=13.6$ eV). Note the discontinuous derivatives at $r = r_0 \approx 6.7$ bohr.

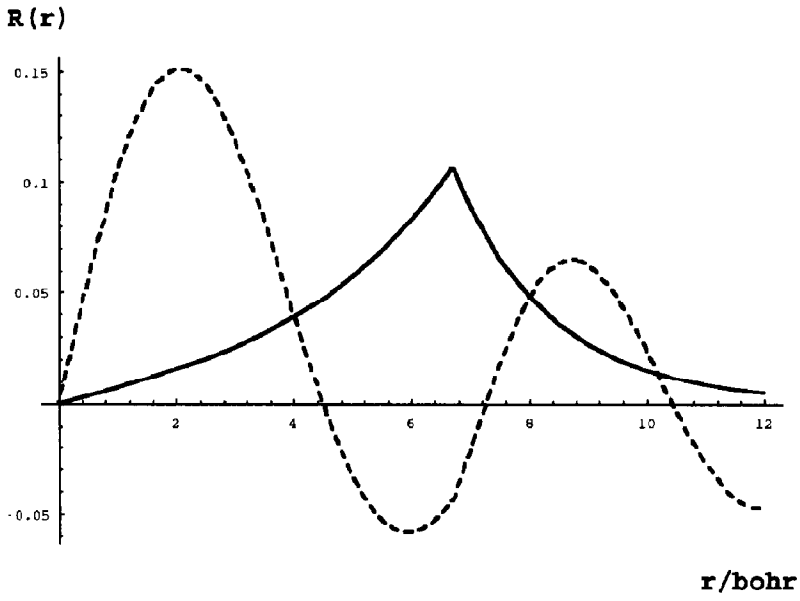

Fig. 2. Radial functions $R(r)$ for bound P state (solid curve) and continuum p state (dashed curve, 1/2 scale) with $k=1$.

discontinuity in the derivative at $r=r_0$, this being necessary to get a deltafunction from the second derivative.

3. Photodetachment cross sections

Differential cross sections for photoelectron processes were derived by Bethe [11]. From the bound s state (designated S) to the p continuum (designated p)

$$\left(\frac{d\sigma}{d\Omega}\right)_s = \frac{2\pi^2 \nu a_0^3}{c} \langle p|r|S\rangle^2 \cos^2\theta . \tag{12}$$

Analogously, from the bound p state (P) to the continuum of s and d states

$$\left(\frac{d\sigma}{d\Omega}\right)_p = \frac{2\pi^2 \nu a_0^3}{9c} [\langle s|r|P\rangle^2 - 2\cos(\delta_2-\delta_0)\langle s|r|P\rangle\langle d|r|P\rangle(3\cos^2\theta-1)+\langle d|r|P\rangle^2(3\cos^2\theta+1)] . \tag{13}$$

In (12) and (13), ν is the radiation frequency and a_0 is the Bohr radius, such that the matrix elements are to be expressed in atomic units. The coordinates θ, ϕ are defined with reference to the direction of polarization of the incident radiation. The magnetic sublevels of the initial state are assumed to be equally populated. With use of the wavefunctions (4) and (9), all of the above matrix elements are real.

The angular dependence of the cross section can be represented in a form suggested by Cooper and Zare [12],

$$\frac{d\sigma}{d\Omega} = \frac{\sigma}{4\pi} [1+\beta P_2(\cos\theta)] , \tag{14}$$

where σ is the total cross section. For photodetachment from an s state

$$\frac{\sigma_s}{4\pi} = \frac{2\pi^2 \nu a_0^3}{3c} \langle p|r|S\rangle^2, \qquad \beta_s = 2 , \tag{15}$$

For a p state, eq. (13) corresponds to

$$\frac{\sigma_p}{4\pi} = \frac{2\pi^2 \nu a_0^3}{9c} [\langle s|r|P\rangle^2 + 2\langle d|r|P\rangle^2] \tag{16}$$

and

$$\beta_p = \frac{2\langle d|r|P\rangle^2 - 4\cos(\delta_2 - \delta_0)\,\langle s|r|P\rangle\langle d|r|P\rangle}{2\langle d|r|P\rangle^2 + \langle s|r|P\rangle^2}. \tag{17}$$

The range of β is -1 to $+2$.

4. Computations

The dipole matrix elements were evaluated analytically as functions of electron energy using Mathematica [#3]. Following are the input formulas:

$$\langle p|r|S\rangle = \left(\int_0^{r_0} + \int_{r_0}^{\infty}\right) R_{k,1}(r) R_{\kappa,0}(r) r^3\,dr$$

$$= N_s\sqrt{2k/\pi}\Bigg[k_0(\kappa r_0)\,[\cos\delta_1 - \sin\delta_1 y_1(kr_0)/j_1(kr_0)] \int_0^{r_0} i_0(\kappa r) j_1(kr) r^3\,dr$$

$$+ i_0(\kappa r_0)\left(\cos\delta_1 \int_{r_0}^{\infty} k_0(\kappa r) j_1(kr) r^3\,dr - \sin\delta_1 \int_{r_0}^{\infty} k_0(\kappa r) y_1(kr) r^3\,dr\right)\Bigg], \tag{18}$$

$$\langle s|r|P\rangle = \left(\int_0^{r_0} + \int_{r_0}^{\infty}\right) R_{k,0}(r) R_{\kappa,1}(r) r^3\,dr$$

$$= N_p\sqrt{2k/\pi}\Bigg[k_1(\kappa r_0)\,[\cos\delta_0 - \sin\delta_0\, y_0(kr_0)/j_0(kr_0)] \int_0^{r_0} i_1(\kappa r) j_0(kr) r^3\,dr$$

$$+ i_1(\kappa r_0)\left(\cos\delta_0 \int_{r_0}^{\infty} k_1(\kappa r) j_0(kr) r^3\,dr - \sin\delta_0 \int_{r_0}^{\infty} k_1(\kappa r) y_0(kr) r^3\,dr\right)\Bigg], \tag{19}$$

$$\langle d|r|P\rangle = \left(\int_0^{r_0} + \int_{r_0}^{\infty}\right) R_{k,2}(r) R_{\kappa,1}(r) r^3\,dr$$

$$= N_p\sqrt{2k/\pi}\Bigg[k_1(\kappa r_0)\,[\cos\delta_2 - \sin\delta_2\, y_2(kr_0)/j_2(kr_0)] \int_0^{r_0} i_1(\kappa r) j_2(kr) r^3\,dr$$

$$+ i_1(\kappa r_0)\left(\cos\delta_2 \int_{r_0}^{\infty} k_1(\kappa r) j_2(kr) r^3\,dr - \sin\delta_2 \int_{r_0}^{\infty} k_1(\kappa r) y_2(kr) r^3\,dr\right)\Bigg]. \tag{20}$$

The cross sections in megabarns (Mb), when the matrix elements are expressed in au, are given by

$$\sigma_s/4\pi = 0.1070(\kappa^2 + k^2)\langle p|r|S\rangle^2, \tag{21}$$

[#3] Software published by Wolfram Research, Inc., Champaign, IL.

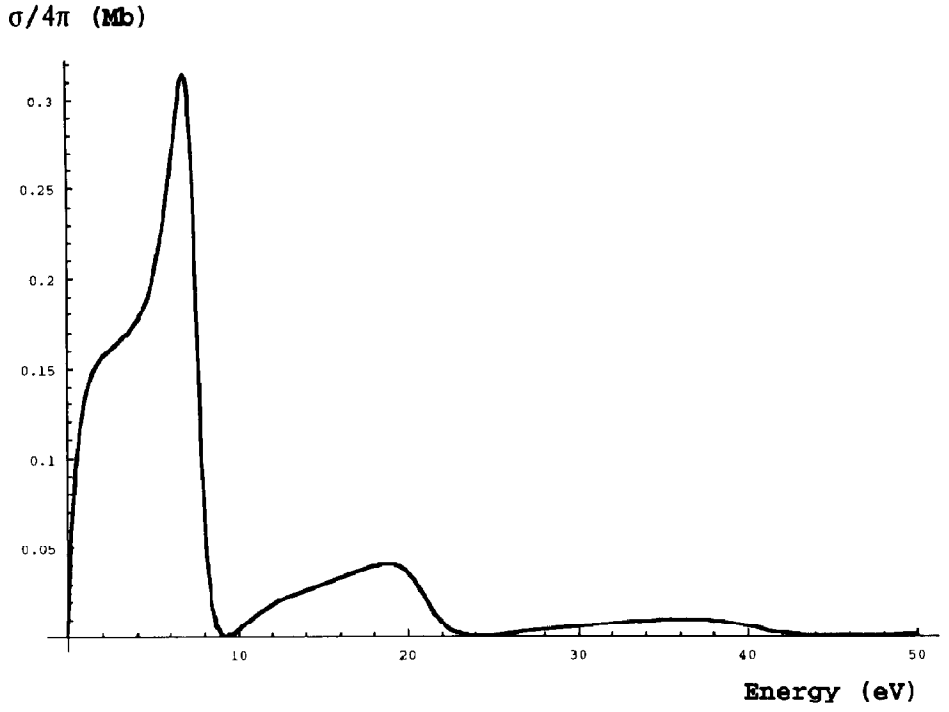

Fig. 3. Average photodetachment cross section versus photoelectron energy from bound S state to continuum p states.

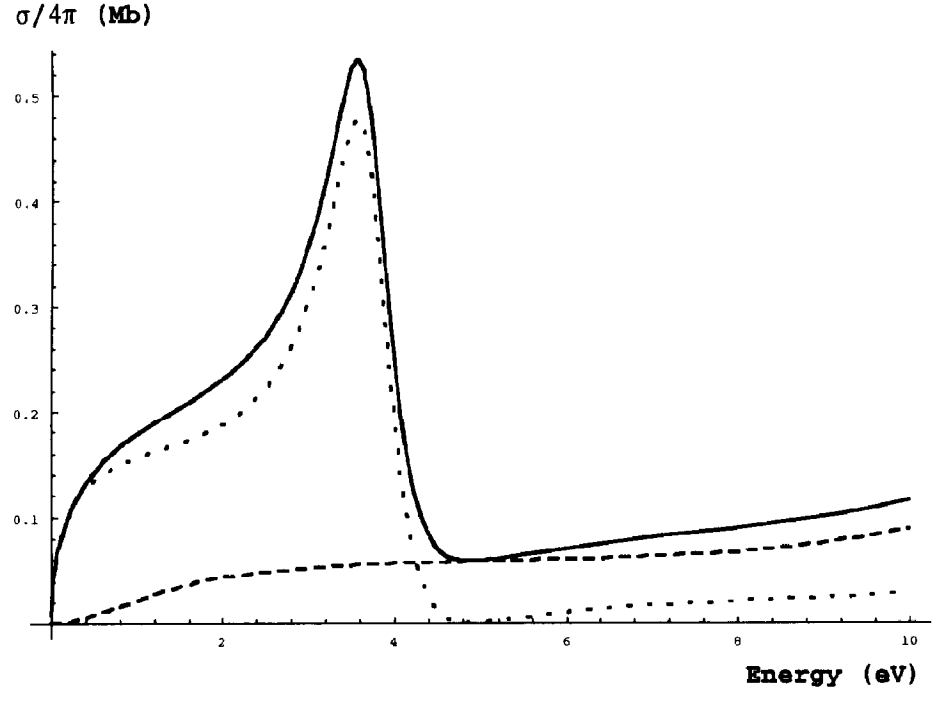

Fig. 4. Average photodetachment cross section versus photoelectron energy from bound P state to continuum s and d states. Dotted curve: P→s contribution; dashed curve: P→d contribution; solid curve: total cross section.

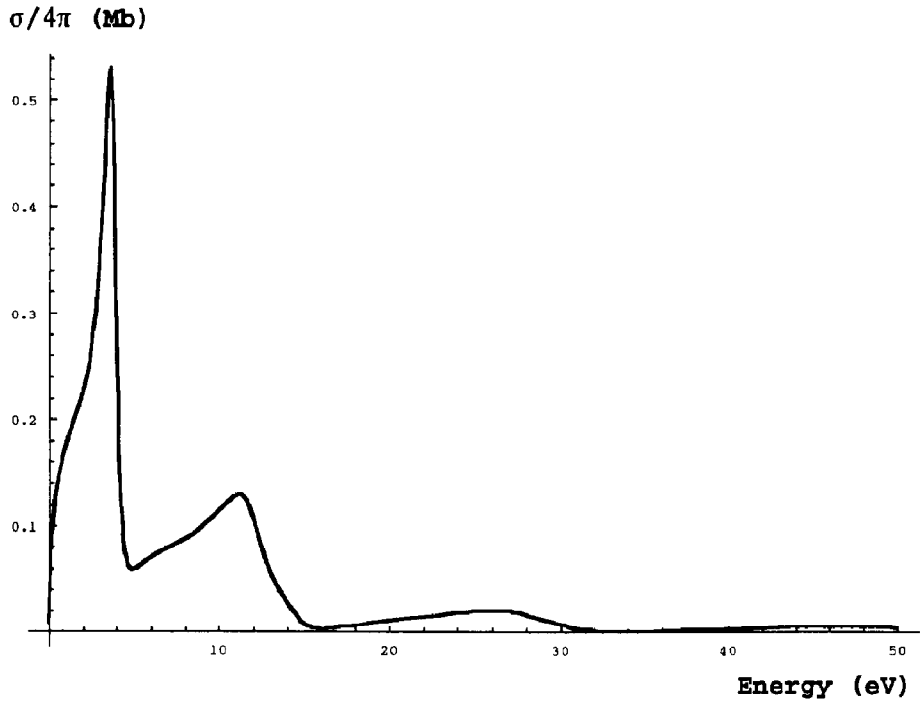

Fig. 5. Cross section versus energy from bound P state on extended energy scale, showing secondary maxima and minima.

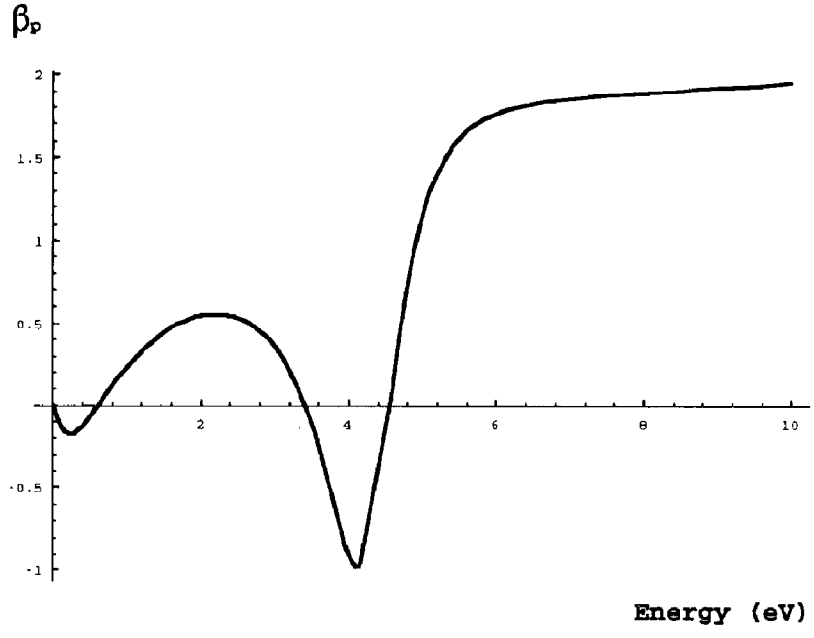

Fig. 6. Asymmetry parameter β_p versus photoelectron energy from P state.

and

$$\sigma_p/4\pi = 0.03567(\kappa^2+k^2)[\langle s|r|P\rangle^2 + 2\langle d|r|P\rangle^2] \,. \tag{22}$$

A note on the dipole-velocity form of the above matrix elements. For exact eigenfunctions, as we have been

using, these ought to give the same photodetachment cross sections as the dipole-length form. This is not precisely true in the present instance, however, because of the discontinuous derivatives of the wavefunctions at $r=r_0$. To demonstrate this, integrate the commutation relation $[\boldsymbol{r}, H]=\mathrm{i}\hbar\boldsymbol{p}$ between two eigenfunctions, say ψ_i and ψ_f. This gives (in au)

$$E_\mathrm{i}\langle \mathrm{f}|\boldsymbol{r}|\mathrm{i}\rangle - \int \psi_\mathrm{f}\left(-\tfrac{1}{2}\nabla^2+\frac{\lambda}{2r_0}\delta(r-r_0)\right)\psi_\mathrm{i}\,\mathrm{d}^3\boldsymbol{r}=\langle \mathrm{f}|\nabla|\mathrm{i}\rangle\,. \tag{23}$$

Integration by parts twice in the second term above turns the Hamiltonian over onto ψ_f, but it also introduces nonvanishing boundary terms. The relation between dipole-length and dipole-velocity matrix elements works out to

$$|\langle \mathrm{f}|\nabla|\mathrm{i}\rangle| = (E_\mathrm{i}-E_\mathrm{f})|\langle \mathrm{f}|\boldsymbol{r}|\mathrm{i}\rangle| + r_0^3[R_\mathrm{f}(r)R_\mathrm{i}'(r)-R_\mathrm{f}'(r)R_\mathrm{i}(r)]_{r0+}^{r0-}\,. \tag{24}$$

However, the boundary terms contribute at most 10^{-4} the magnitude of the $\boldsymbol{r}$ and ∇ matrix elements and thus are entirely negligible.

5. Results and discussion

For reference purposes we show in fig. 3 the average cross section $\sigma_\mathrm{s}/4\pi$ plotted as a function of photoelectron energy for S→p transitions. The asymmetry parameter β_s has the constant value 2 for this case. In common with an analogous atomic photodetachment process (e.g. $\mathrm{H}^-\rightarrow\mathrm{H}$), the cross section increases from zero at threshold to a maximum, then decreases. An anomaly, however, is the non-monotonic decay of σ_s. In fact, the cross section goes through a nearly periodic pattern of zeros. This behavior has an analog in the scattering of electromagnetic waves from a conducting sphere (see, for example, ref. [13]), considering only the electric part of the radiation field. In this instance, scattering maxima occur for values of the radiation wavenumber given by $k=n\pi/r_0$, $n=1, 2, 3, \ldots$.

Of greater relevance for C_{60}^- is the process P→s+d, which models the photodetachment from the t_{1u} SUMO. The average cross section as a function of photoelectron energy is shown in figs. 4 and 5. The asymmetry parameter β_p is likewise plotted as a function of photoelectron energy in fig. 6.

We note in fig. 5 cross section maxima and minima similar to those in fig. 3 for the S→p process. However, while the minima for S→p correspond to zero values of cross section, those for P→s+d are nonzero minima because of the overlap of two final-state channels. Note also in fig. 6 that β_p passes through zero at several values of photoelectron energy below 5 eV. While the zero value of β_p at threshhold corresponds to a vanishing of the P→d matrix element, the other zeros reflect destructive interference between the two photodetachment channels.

The photodetachment of a t_{1u} electron from the SOMO of C_{60}^-, as modeled by the ejection of an $l=1$ electron from the attractive Dirac bubble potential, resembles the detachment of a p electron from an atomic anion such as a halide (see, for example, ref. [14]), for example, $\mathrm{Cl}^-\rightarrow\mathrm{Cl}+\mathrm{e}$. In both instances, interference between s- and d-photoelectron channels is exhibited. The novel feature for the fullerene is the appearance of secondary maxima and minima in the cross section.

References

[1] S.M. Blinder, Chem. Phys. Letters 64 (1979) 485.
[2] T. Kajiwara, K. Funabashi and C. Naleway, Phys. Rev. A 6 (1972) 808.
[3] S.H. Yang, C.L. Pettiette, J. Conceicao, O. Cheshnovsky and R.E. Smalley, Chem. Phys. Letters 139 (1987) 233.
[4] R.C. Haddon, L.E. Brus and K. Raghavachari, Chem. Phys. Letters 125 (1986) 459.
[5] S. Larsson, A. Volosov and A. Rosén, Chem. Phys. Letters 137 (1987) 501.
[6] J. Guo, D.E. Ellis and D.J. Lam, Chem. Phys. Letters 184 (1991) 418.

[7] M.R. Savina and A.H. Francis, private communication.
[8] M. Abramowitz and I.A. Stegun, eds., Handbook of mathematical functions NBS (US GPO, Washington, 1972) p. 443.
[9] S. Liu, Y.-J. Lu, M.M. Kappes and J.A. Ibers, Science 254 (1991) 408.
[10] K. Hedberg, L. Hedberg, D.S. Bethune, C.A. Brown, H.C. Dorn, R.D. Johnson and M. de Vries, Science 254 (1991) 410.
[11] H.A. Bethe, Handbuch der Physik, Vol. 24/1 (Springer, Berlin, 1933) pp. 483, 484;
S.H. Lin, Can. J. Physics 46 (1968) 2719, and references therein.
[12] J. Cooper and R.N. Zare, J. Chem. Phys. 48 (1968) 942; 49 (1968) 4252 (E).
[13] M. Kerker, Scattering of light and other electromagnetic radiation (Academic Press, New York, 1969) pp. 97ff.
[14] M. Mohraz and L.L. Lohr, Intern. J. Quantum Chem. 10 (1976) 811, and references therein.